The Dual-Specific Active Site of 7,8-Diaminopelargonic Acid Synthase and the Effect of the R391A Mutation[†]

Andrew C. Eliot,[‡] Jenny Sandmark,[§] Gunter Schneider,[§] and Jack F. Kirsch*,[‡]

Department of Chemistry, University of California−Berkeley, Berkeley, California 94720-3206, and Department of Medical Biochemistry and Biophysics, Karolinska Institutet, S-171 77 Stockholm, Sweden

ABSTRACT: 7,8-Diaminopelargonic acid (DAPA) synthase (EC 2.6.1.62) is a pyridoxal phosphate (PLP)-dependent transaminase that catalyzes the transfer of the α-amino group from S-adenosyl-L-methionine (SAM) to 7-keto-8-aminopelargonic acid (KAPA) to form DAPA in the antepenultimate step in the biosynthesis of biotin. The wild-type enzyme has a steady-state k_{cat} value of 0.013 s^{-1}, and the K_m values for SAM and KAPA are 150 and <2 μM, respectively. The k_{max} and apparent K_m values for the half-reaction of the PLP form of the enzyme with SAM are 0.016 s^{-1} and 300 μM, respectively, while those for the reaction with DAPA are 0.79 s^{-1} and 1 μM. The R391A mutant enzyme exhibits near wild-type kinetic parameters in the reaction with SAM, while the apparent K_m for DAPA is increased 180-fold. The 2.1 Å crystal structure of the R391A mutant enzyme shows that the mutation does not significantly alter the structure. These results indicate that the conserved arginine residue is not required for binding the α-amino acid SAM, but it is important for recognition of DAPA.

Biotin (vitamin H) is a vitamin that is essential to all organisms as a carrier of activated carbon dioxide, but it is synthesized only in plants, microorganisms, and some fungi (for recent reviews, see refs *4* and *5*). All other organisms must obtain biotin in their diet or from intestinal bacteria. Because this biosynthetic pathway is not present in humans, it is an attractive target for antibiotics and herbicides. A better understanding of the enzymes involved in this pathway is crucial for the development of such compounds.

7,8-Diaminopelargonic acid (DAPA)[1] synthase from *E. coli* is a pyridoxal phosphate (PLP) dependent aminotransferase that catalyzes the second of four steps in biotin biosynthesis (Scheme 1, *6*). In this step, the α-amino group from S-adenosylmethionine (SAM) is transferred to 7-keto-8-aminopelargonic acid (KAPA), converting it to DAPA. This enzyme is the only aminotransferase known to utilize SAM as an amino donor. The mechanism of this reaction is

the same as for other PLP-dependent aminotransferases and is shown in Scheme 2. DAPA synthase was first purified in 1975 (*7*), and a limited kinetic characterization was published the same year (*8*). Recently, the three-dimensional structures of the PLP-bound holoenzyme and a nonproductive complex of the PLP form of the enzyme with the keto-acid substrate KAPA were determined by X-ray crystallography (*3*). The structure analysis verified that DAPA synthase belongs to the fold type I of aminotransferases and identified residues involved in cofactor and substrate binding. Arg391, which has been aligned with Arg386 of aspartate aminotransferase (AATase; EC 2.6.1.1) in one sequence alignment (*9*) but is not structurally analogous (*10*), forms hydrogen bonds to the terminal carboxylate of KAPA. Arg386 (AATase numbering) is structurally conserved among all other aminotranferases that utilize α-amino acids as substrates, but is missing in DAPA synthase.

Here we report the kinetic characterization of the WT enzyme. The intriguing fact that two substrates, which are very different in size and in the distance between the carboxylate and the amino group that condenses with PLP (one carbon in SAM and six carbons in KAPA), bind in the same active site prompted an investigation of the effects of the mutation of Arg391 to alanine on the reaction with each substrate. The crystal structure of the R391A mutant was determined to assess the impact on the structure.

EXPERIMENTAL PROCEDURES

Reagents. The sulfate salt of DAPA was synthesized by the method of duVigneaud et al. (*11*). The hydrochloride salt of KAPA was synthesized by the method of Nudelman et al. (*12*).[2] Unless otherwise noted, the commercially available sulfate salt of SAM (a mixture of ∼60% (*S,S*) and 40% (*R,S*) diastereomers) was used without further purifica-

* To whom correspondence should be addressed. Telephone: (510) 642-6368. Fax: (510) 642-6368. E-mail: jfkirsch@uclink4.berkeley.edu.
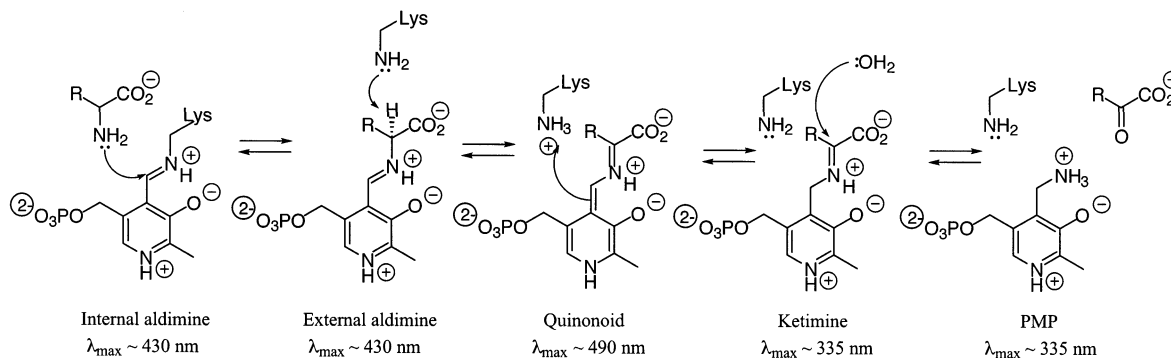‡ University of California−Berkeley.
§ Karolinska Institutet.

[1] Abbreviations: AATase, aspartate aminotransferase; ACC, 1-aminocyclopropane-1-carboxylate; AMPSO, N-(1,1-dimethyl-2-hydroxyethyl)-3-amino-2-hydroxypropanesulfonic acid; ATase, aminotransferase; ATP, adenosine 5′-triphosphate; CAPS, 3-(cyclohexylamino)-1-propanesulfonic acid; DAPA, 7,8-diaminopelargonic acid; EDTA, ethylenediaminetetraacetate; GABA, γ-aminobutyric acid; GSA, glutamate 1-semialdehyde aminomutase; HEM buffer, 50 mM HEPES, 0.1 M EDTA, 10 mM β-mercaptoethanol; HEPES, N-(2-hydroxyethyl)-piperazine-N′-(2-ethanesulfonic acid); KAPA, 7-keto-8-aminopelargonic acid; PLP, pyridoxal 5′-phosphate; PMP, pyridoxamine 5′-phosphate; rmsd, root mean-squared deviation; SAM, S-adenosyl-L-methionine; TAPS, N-[tris(hydroxymethyl)methyl]-3-aminopropane sulfonic acid; WT, wild-type.

Scheme 1: Biotin Biosynthetic Pathway in *E. Coli*[a]
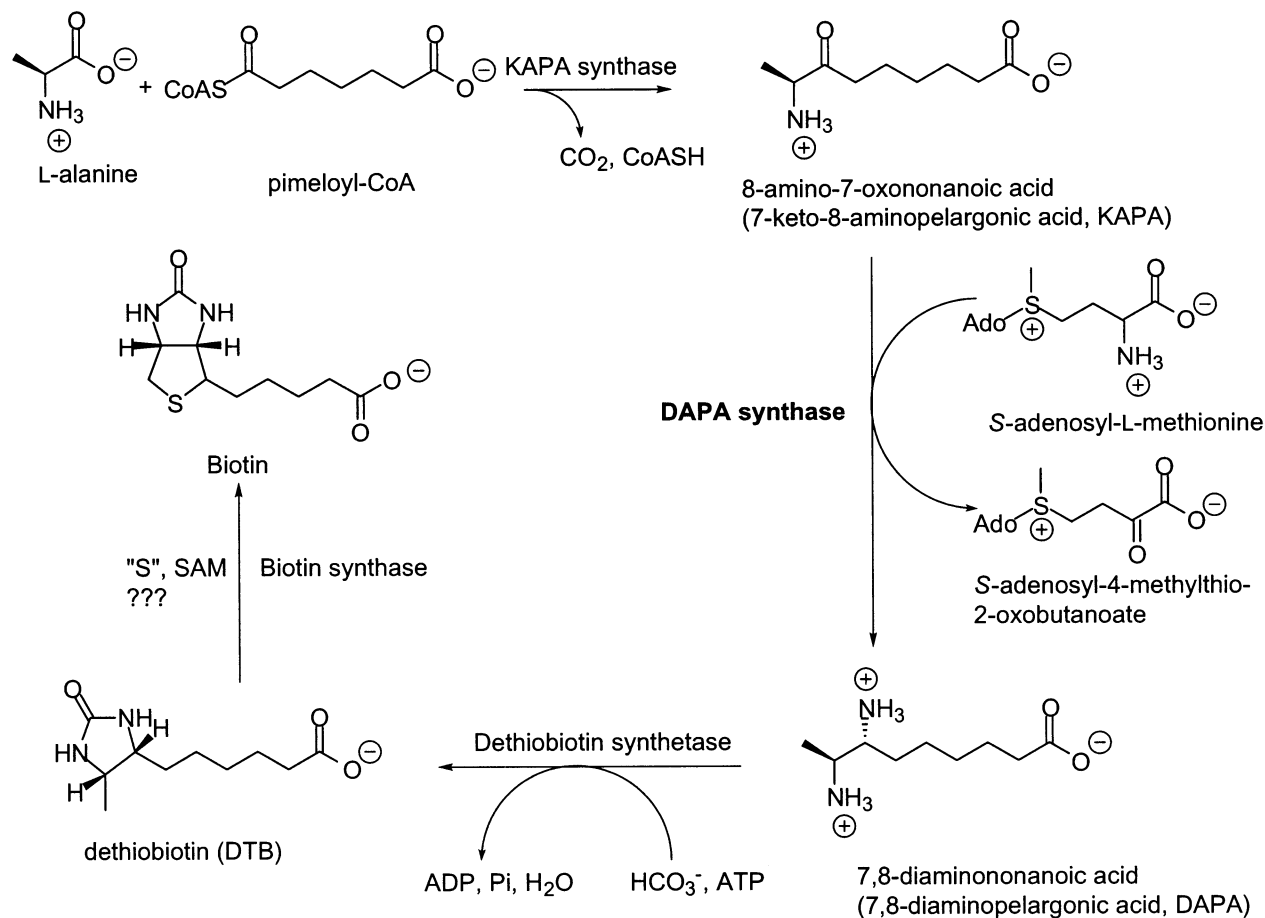
[a] From refs *4* and *5*. Neither the stoichiometry nor the mechanism of biotin synthase is known.

Scheme 2: Mechanism of an Aminotransferase Half-Reaction[a]

Internal aldimine	External aldimine	Quinonoid	Ketimine	PMP
$\lambda_{max} \sim 430$ nm	$\lambda_{max} \sim 430$ nm	$\lambda_{max} \sim 490$ nm	$\lambda_{max} \sim 335$ nm	$\lambda_{max} \sim 335$ nm

[a] To restore the PLP of the enzyme, the enzyme reacts with a keto acid in the reverse of the reaction shown.

tion. Diastereometrically pure (*R,S*)- and (*S,S*)-SAM were produced as described in (*13*). All other reagents are commercially available.

Overexpression and Purification of WT and R391A DAPA Synthase. WT and R391A DAPA synthase were both expressed from the pT7bioA plasmid and purified as previously described (*14*). The R391A mutation was introduced into the plasmid with the QuikChange kit (Stratagene). The entire insert was sequenced to ensure the absence of other mutations.

Spectrophotometric pH Titration of WT DAPA Synthase. A solution of DAPA synthase in HEM buffer (50 mM HEPES, 0.1 mM EDTA, 10 mM β-mercaptoethanol, pH 7.5) was diluted into a buffer containing 5 mM TAPS, 20% glycerol, and 0.5 M KCl, pH 7.5, to a final enzyme concentration of 15 μM. The initial pH of 7.6 was adjusted by addition of 0.5 M AMPSO, pH 10.7 (final pH 7.6−9.9), 0.5 M CAPS, pH 11.5 (final pH 10−10.7), and 0.5 M TAPS, pH 13.0 (final pH 10.8−11.9). Spectra were recorded from 250 to 500 nm on a UVIKON 360 double-beam spectrophotometer (KONTRON Instr.). The absorbances at the

---

[2] Contrary to the report cited, this procedure yielded a mixture of enantiomers, most likely as a result of racemization during the final step. Lucet et al. (*1*) have observed racemization under similar conditions.

wavelengths of maximum difference (430 and 345 nm) were plotted as a function of pH (Figure 1), and the data were fitted to eq 1a (A_{430}) or 1b (A_{345}) using Kaleidagraph (Synergy Software, Reading, Pa.), where A_1 and A_2 are the maximum and minimum absorbance values, respectively:

$$A = \frac{A_1 - A_2}{1 + 10^{(pH - pK_a)}} + A_2 \qquad (1a)$$

$$A = \frac{A_1 - A_2}{1 + 10^{(pK_a - pH)}} + A_2 \qquad (1b)$$

The Single-Turnover Reaction of DAPA Synthase with SAM. WT DAPA synthase (4.5 μM) was incubated with varying concentrations of SAM (10–1000 μM) in reaction buffer (50 mM AMPSO, 20% glycerol, pH 9.0) in a total volume of 150 μL. The absorbance spectra from 250 to 550 nm were recorded at 5 s intervals for 400 s on a Hewlett-Packard 8453 single-beam diode-array spectrophotometer. The rate constants for the appearance of the product absorbance at 330 nm were determined by nonlinear regression with the Chemstation software provided with the instrument. To determine the rate constant for the formation of the quinonoid intermediate, a solution of 2 mM SAM in reaction buffer was mixed 1:1 with a solution of 30 μM DAPA synthase in reaction buffer in a total volume of 100 μL, and the absorbance at 500 nm was recorded at 0.5 ms intervals for 200 ms on an Applied Photophysics Ltd. SF17.MV stopped-flow spectrophotometer. The data were fit to a first-order curve using Kaleidagraph. The k_{max} and apparent K_m values for the half-reactions were determined by plotting the observed rate constants versus SAM concentration and fitting the data to eq 2 (*15*), where k_r is a term that represents the contribution of the reverse reaction:

$$k_{obs} = \frac{k_{max}[S]}{K_m{}^{app} + [S]} + k_r \qquad (2)$$

Although k_r is not a constant (*16*), it does not vary significantly over the range of substrate concentrations used in these experiments.

Single-Turnover Reaction of DAPA Synthase with DAPA. A solution of 0.5 μM DAPA synthase in reaction buffer was mixed 1:1 with solutions containing various concentrations of DAPA in reaction buffer in a total volume of 100 μL. The fluorescence emission at wavelengths > 360 nm was measured with an Applied Photophysics Ltd. SF17.MV stopped-flow spectrophotometer equipped for fluorescence detection. The 280 nm excitation wavelength results in excitation of the 335 nm-absorbing PMP chromophore via energy transfer from excited tyrosine and tryptophan residues (*17*). Data at multiple wavelengths were acquired on a Hi-Tech Scientific SF61-DX2 diode-array stopped-flow spectrophotometer. The k_{max} and apparent K_m values were determined by globally fitting all of the data to the model shown in Scheme 3 with the Dynafit software package (*18*).

HPLC Assay for Production of DAPA. WT DAPA synthase (1.5 μM) was incubated with varying concentrations of D,L-KAPA and SAM in reaction buffer at 25 °C in a total volume of 1 mL. At selected time points, 200 μL aliquots were removed and quenched by addition of 10 μL of 100% trichloroacetic acid. After 30 min at −20 °C, the precipitated
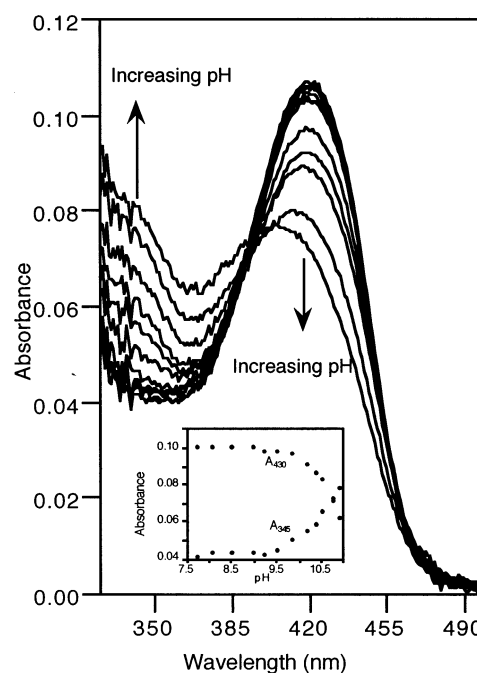

FIGURE 1: pH dependence of the absorption spectra of DAPA synthase. DAPA synthase was diluted to 15 μM in HEM buffer (50 mM HEPES, 0.1 mM EDTA, 10 mM β-mercaptoethanol) with an initial pH of 7.5. Spectra were recorded at 25 °C at pH 7.74, 8.06, 8.52, 9.01, 9.23, 9.52, 9.86, 10.21, 10.40, 10.57, 10.77, and 10.91. (Inset) The absorption at 430 and 345 nm vs pH.

Scheme 3: Kinetic Model for the Reaction of DAPA Synthase with DAPA

$$\text{Enz} \underset{k_{-1}}{\overset{k_1[S]}{\rightleftharpoons}} \text{E-S} \overset{k_2}{\longrightarrow} \text{E-P}$$
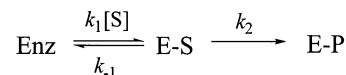
enzyme was removed by centrifugation for 10 min at 10 000g. The pH of the supernatant was adjusted to 10 by addition of 12 μL 6.5 N NaOH. The DAPA was derivatized by a modified version of the procedures described by Roth (*19*) and Contestabile et al. (*20*). In brief, 22 μL of 1 M sodium carbonate, pH 10.0, was added to the supernatant from the previous step, followed by 40 μL of phthalic dicarboxaldehyde (20 mg/mL) and β-mercaptoethanol (10 μL/mL) in 95% ethanol, and the resulting mixture was kept for at least 1 h at 25 °C. This mixture was then injected onto an Alltech Nucleosil C18 HPLC column run isocratically in 43% acetonitrile and 1% acetic acid with a Varian ProStar HPLC system. The derivatized DAPA, which absorbs at 420 nm, eluted 17 min after the injection. The concentration of DAPA was determined from a standard curve generated from authentic samples of DAPA in reaction buffer. The standard samples were treated exactly as the reaction aliquots. The initial rates for the steady-state reactions were determined by linear fits of plots of the quantity of DAPA produced versus time. These initial rates were then plotted against substrate concentration and fit to the Michaelis–Menten equation to determine the steady-state kinetic parameters.

Crystallization of the R391A Mutant Protein. The R391A mutant was crystallized as described by Käck et al. (*14*), with the modification that 2-propanol was added to the crystallization mixture to a final concentration of 0.4 M. WT crystals belonging to the space group $P2_1$ were used for

Table 1: Data Collection and Refinement Statistics

wavelength (Å)	1.12
resolution (Å)	20.0−2.10 (2.21−2.10)[a]
R_{sym} (%)	6.8 (16.8)
I/σ	15.8 (5.3)
completeness (%)	99.2 (97.2)
no. of reflections	177 643
unique reflections	43 771
$R_{refinement}$ (%)	20.1
R_{free} (%)	23.3
B factor (Å^2)	
protein atoms	32.5
cofactor	24.5
water	38.7
2-propanol	57.6
root-mean-square deviation	
bonds (Å)	0.013
angles (deg)	1.4
Ramachandran plot, residues in	
most favorable regions (%)	89.6
additional allowed regions (%)	9.5
generously allowed regions	0.3
disallowed regions (%)	0.7

[a] Values in parentheses are data for the highest resolution shell.

microseeding to induce nucleation. The R391A protein crystallized in space group C2 with the cell dimensions, a = 127.9 Å, b = 55.9 Å, c = 116.2 Å, β = 110.1°, with the dimer in the asymmetric unit.

Structure Determination. Data were collected using a Marresearch 165 mm CCD detector at beamline I711 at MAX-lab (Lund University, Sweden) and processed with MOSFLM (*21*) and SCALA (*22*). Details on data collection are presented in Table 1. The structure was solved by molecular replacement (Amore, *23*) with the WT enzyme dimer as the search model. The initial electron density map showed negative density for the Arg391 side chain (Figure 5), and the residue was subsequently replaced by alanine in the model. Refinement was performed using Refmac5 (*24*) and 5% of the reflections were excluded to monitor R_{free}. Water molecules were added to the model and inspected manually during refinement. The O software (*25*) was used for manual rebuilding. The quality of the model was assessed with PROCHECK (*26*). A strong difference electron density in the active site close to the PLP was interpreted as a 2-propanol molecule because the observed size and shape of the electron density fits well with this molecule, which is present in the crystallization mixture in high concentration. No other compound present in the crystallization mixture would fit equally well. Statistics of the refinement and the resulting model are given in Table 1. Three residues in each subunit, Lys274, Ile213, and one conformation of Trp53, are found in the disallowed regions of the Ramachandran plot. These three residues are well defined in the electron density map and also appear in the disallowed regions in the WT structure. Two stretches of disordered residues are observed in both subunits (159−168 and 180−189). These residues are situated in two loop regions at the surface of the protein and are also poorly defined in the WT structure. The refined model consists of residues 1−182 and 184−428, one PLP molecule, one sodium ion, and one 2-propanol molecule per subunit and 342 water molecules. The coordinates and structure factors have been deposited in the Protein data bank with the accession number 1mgv.

Scheme 4: Typical Wavelengths of Maximum Absorbance of the Acidic and Basic Forms of the Internal Aldimine Formed with Pyridoxal 5′-Phosphate

Protonated internal aldimine
$\lambda_{max} \sim 430$ nm

Deprotonated internal aldimine
$\lambda_{max} \sim 360{-}390$ nm
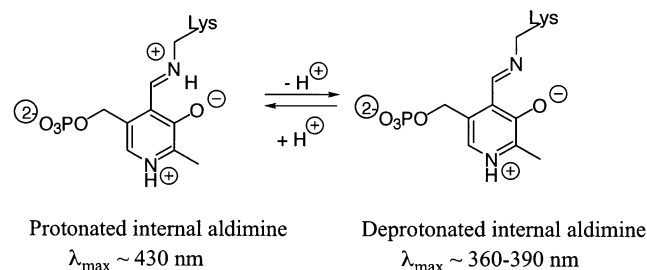
RESULTS

Spectrophotometric pK_a of the Internal Aldimine of DAPA Synthase is >10.5. At neutral pH, the PLP cofactor of DAPA synthase exhibits an absorbance at 430 nm characteristic of a protonated internal aldimine (Scheme 4). The crystal structure shows that the aldimine is formed with Lys274 (*3*). The pK_a of the aldimine was determined by spectrophotometric titration to be >10.5 (Figure 1).

Kinetic Parameters for the Single-Turnover Transamination of DAPA Synthase with SAM. The 430 nm absorbance peak of the PLP form of DAPA synthase is converted to 335 nm, characteristic of a ketimine or the pyridoxamine (PMP) form of the enzyme, when SAM is added. The k_{max} and apparent K_m values for this half-reaction are 0.016 s^{-1} and 300 μM (Table 2), respectively. A strong transient absorbance at 487 nm, attributed to a quinonoid intermediate, was observed during the reaction (Figure 2). This species decays with a rate constant equal to k_{max}. The rate constant for the formation of this intermediate measured with a stopped-flow spectrophotometer is 47 s^{-1} (Table 3).

The Enzyme is Specific for (S,S)-SAM. DAPA synthase does not exhibit any spectral change when incubated with excess (R,S)-SAM; nor is this nonbiological diastereomer an inhibitor of the single-turnover reaction with the natural diastereomer (S,S)-SAM (data not shown).

Kinetic Parameters for the Single-Turnover Transamination of DAPA Synthase with DAPA. The 430 nm absorbance peak of the PLP form of DAPA synthase is converted to 335 nm when DAPA is added (Figure 3). No intermediate is observed. The 335 nm species also fluoresces at 390 nm when excited at 335 or 280 nm. The appearance of the product was therefore followed by fluorescence detection (λ_{ex} = 280 nm) on a stopped-flow spectrophotometer. The plot of fluorescence intensity versus time exhibits a distinct sigmoidal shape when the kinetics are initiated with DAPA concentrations below 4 μM (Figure 4), consistent with two consecutive first-order reactions, the first of which is reversible (Scheme 3). By analogy to the steady-state Michaelis−Menten equation, $k_{max} = k_2$ and the apparent K_m is $(k_2 + k_{-1})/k_1$. The best-fit values for the microscopic rate constants in this model are $k_1 = 9.1 \times 10^5$ M^{-1} s^{-1}, $k_{-1} = 0.16$ s^{-1}, and $k_2 = 0.79$ s^{-1}, respectively (Table 3). The calculated k_{max} and apparent K_m values are thus 0.79 s^{-1} and 1 μM, respectively (Table 2).

New Assay for the Steady-State Reaction of DAPA Synthase. Previous studies of DAPA synthase made use of a bioassay, which monitors the growth of an auxotroph in

Table 2: Michaelis-Menten Parameters for the Steady-State and Single-Turnover Half-reactions of WT and R391A DAPA Synthase

	steady-state				half-reactions			
	k_{cat} (s^{-1})	K_m^{KAPA} (μM)	K_m^{SAM} (μM)	K_i^{KAPA} (μM)	$k_{max}(SAM)$ (s^{-1})	$K_m^{app}(SAM)$ (μM)	$k_{max}(DAPA)$ (s^{-1})	$K_m^{app}(DAPA)$ (μM)
WT	0.013	<2	150	25[a]	0.016	300	0.79	1.0
	$(0.001)^b$		(50)		(0.004)	(50)	(0.01)	(0.1)
R391A	0.0021	230	50	>2000	0.014	70	0.56	180
	(0.0003)	(10)	(5)		(0.002)	(20)	(0.02)	(30)

[a] Ref 8. [b] Values in parentheses are the calculated errors.
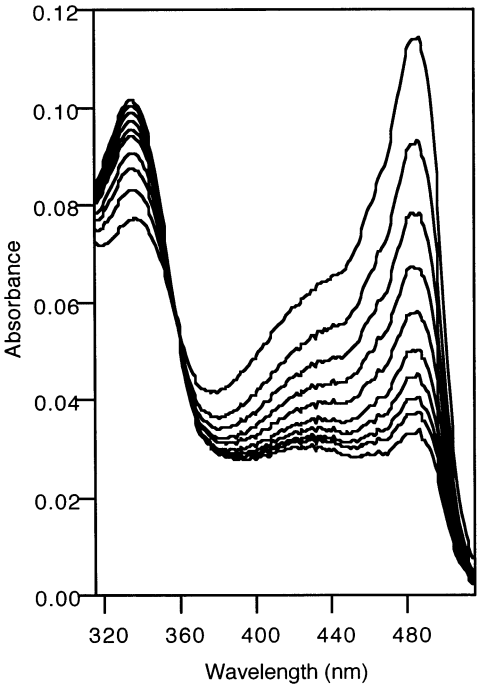

FIGURE 2: Time course of the reaction of 4.5 μM DAPA synthase with 1 mM SAM at 25 °C. Spectra were recorded every 30 s. The strong absorbance at 485 nm is characteristic of a quinonoid intermediate. The isosbestic point at 360 nm indicates that there are only two species present. The reaction buffer was 50 mM AMPSO, 20% glycerol, pH 9.0.

Table 3: Some Microscopic Rate Constants for the Half-Reactions of WT DAPA Synthase

$k_1{}^a$	9.1 ($\pm$ 0.2) $\times$ 10^5 M^{-1} s^{-1}
k_{-1}	0.16 $\pm$ 0.02 s^{-1}
k_2	0.79 $\pm$ 0.01 s^{-1}
$k_Q{}^b$	47 $\pm$ 1 s^{-1}

[a] k_1, k_{-1}, and k_2 are the microscopic rate constants for reaction with DAPA as shown in Scheme 3. [b] k_Q is the first-order rate constant for the formation of the quinonoid intermediate in the reaction with SAM (Scheme 2).

response to DAPA (*27*). We have developed an HPLC-based assay, in which the product DAPA is derivatized with phthalic dicarboxaldehyde after the methods of Contestabile et al. (*20*) and Roth (*19*). This assay is more quantitative than the bioassay, although it is less sensitive. The bioassay is reported to detect DAPA concentrations as low as 0.5 μM (*27*), while the HPLC assay is accurate only for concentrations greater than 2 μM. The steady-state k_{cat} value for the reaction of DAPA synthase with the physiological substrates SAM and KAPA determined with this assay is 0.013 s^{-1}. The steady-state K_m value for SAM is 150 μM. The steady-state K_m value for KAPA could not be determined because of the low sensitivity of the assay, but it is less than 2 μM.
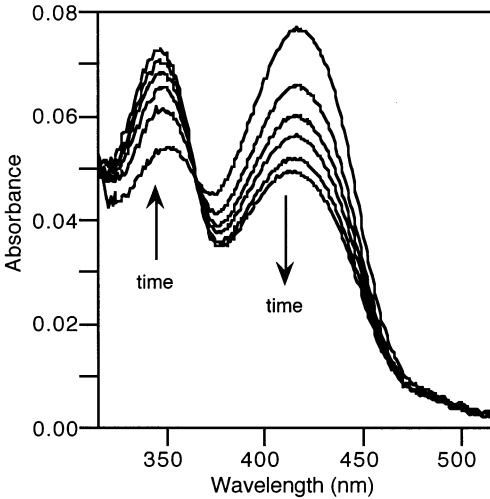

FIGURE 3: Time course of the reaction of 2.5 μM DAPA synthase with 25 μM DAPA at 25 °C. Spectra were recorded at 0.1, 0.4, 0.7, 1.0, 1.5, and 2.0 s. The clean isosbestic point and the lack of a peak at 485 nm indicate that no intermediate accumulates during the reaction. The reaction buffer was 50 mM AMPSO, pH 9.0.
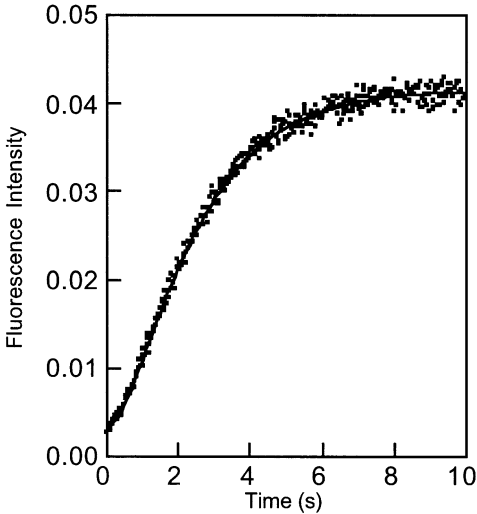

FIGURE 4: Time course of the reaction of 250 nM DAPA synthase with 1 μM DAPA. Fluorescence intensity was recorded every 25 ms for 10 s. The solid line represents a fit to the model shown in Scheme 3. The reaction buffer was 50 mM AMPSO, pH 9.0.

The reaction is inhibited by high KAPA concentrations, as reported (K_i = 25 μM; *8*), because of the formation of a dead-end complex of KAPA with the PLP form of the enzyme.

R391A Mutation Increases the Apparent K_m Value for DAPA 180-Fold. The R391A mutant has a single-turnover K_m^{app} for DAPA of 180 μM compared to 1 μM for the WT. The k_{max} is slightly less than that of WT (0.79 vs 0.56 s^{-1}). The net decrease in k_{max}/K_m^{app} is thus 250-fold. This mutation
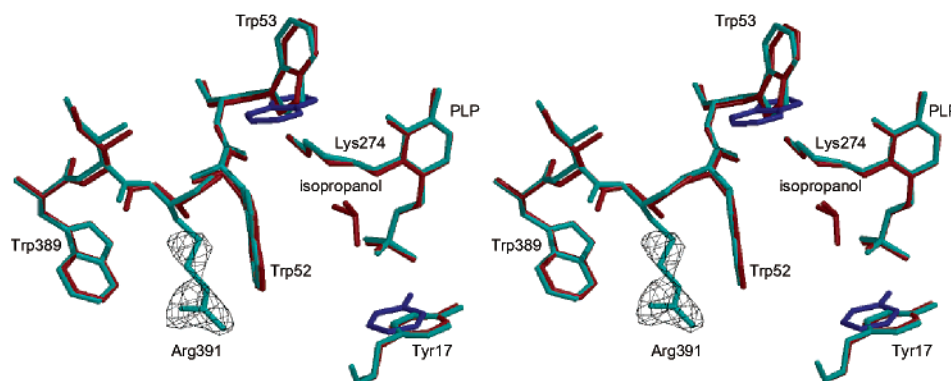
FIGURE 5: Superposition of the structures of WT DAPA synthase (cyan) and the R391A mutant (red). The double conformations observed for Tyr17 and Trp53 in the R391A structure are depicted in red and blue. The initial $F_o - F_c$ map at -3.0 σ contour level is shown in order to illustrate the R391A mutation. This figure was generated using BOBSCRIPT (*43, 44*) and RASTER3D (*45*).

also results in a *decrease* in the single-turnover K_m^{app} value for SAM from 300 μM to 70 μM. The k_{max} value is unchanged; thus, the net increase in k_{max}/K_m^{app} for SAM is 4-fold.

The effect of the mutation on the steady-state kinetic parameters is more pronounced. The K_m value for KAPA is increased from <2 μM to 230 μM, while K_m^{SAM} is reduced from 150 μM to 50 μM, similar to the single-turnover values, but k_{cat} is decreased from 0.013 to 0.0021 s^{-1}. The dead-end K_i for KAPA is much larger than the WT value. The large reduction in the steady-state k_{cat} as compared to the single-turnover k_{max} values suggests that the release of one of the products, a step not observable in the single-turnover reaction, is at least partially rate-limiting. The kinetic parameters for the WT and R391A mutant enzymes are collected in Tables 2 and 3.

Crystal Structure of the R391A DAPA Synthase Mutant. The overall structure of the R391A mutant, determined to 2.1 Å resolution, is similar to that of the WT enzyme (*3*) with an rmsd from WT C$_\alpha$ positions of 0.25 Å.

To obtain crystals of R391A, we used microseeding with WT crystals belonging to space group $P2_1$. The resulting crystals grew in space group C2. DAPA synthase has been observed to crystallize in both space groups and even to change between the two during data collection (*14*).

In the mutant structure a 2-propanol molecule is found in the KAPA binding site of the WT complex. The side chains of Trp53 and Tyr17 adopt double conformations (Figure 5). One corresponds to the position of these side chains in the unliganded enzyme, whereas the second is that seen in the enzyme-KAPA complex (*3*). It may be that the binding of 2-propanol in the KAPA site induces the same side chain movements that were observed upon substrate association. The double conformations would then be the result of partial occupancy by 2-propanol. The high *B* factors for the 2-propanol molecules relative to the rest of the enzyme (Table 1) are also consistent with the sites not being fully occupied. The high structural similarity between WT and mutant enzymes suggests that the kinetic data are not compromised by structural changes as a result of the amino acid replacement. It is not surprising that the removal of the side chain of Arg391 has no structural effects since the only interaction between its guanidino group and the rest of the enzyme is a single hydrogen bond to Gln380, a residue that is well anchored by other hydrogen bonds. The bond between Gln380 and Arg391 is broken when KAPA binds with no resultant movement of Gln380.

DISCUSSION

pK$_a$ of the Internal Aldimine of DAPA Synthase is > 10.5. Transaldimination reactions require that the nucleophilic amine is in the free base form and that the electrophilic imine be protonated; therefore, in the optimum case of a diffusion-controlled reaction, the imine must be more basic than the incoming amine, and the amine must have a pK$_a$ near or below physiological pH. Were this not so, the second-order rate constant would be reduced by the ratio $1/(10^{pH-pK_1} + 10^{pK_2} - pH + 1)$, where pK$_1$ and pK$_2$ are the pK$_a$ values for the free enzyme aldimine and free substrate amine, respectively. Thus, in the diffusion-controlled reaction of the PLP-dependent enzyme 1-aminocyclopropane-1-carboxylate (ACC) synthase (EC 4.4.1.14) with its substrate SAM, the pK$_a$'s of SAM and the internal aldimine are 7.8 (*28*) and 9.3 (*29*), respectively. Mutations that lower the enzyme pK$_a$ reduce the second-order rate constant (*30*). The prototropic groups of DAPA synthase superficially resemble those of ACC synthase in that the substrate amino group pK$_a$'s are low (DAPA = 6.8, *31*), and the internal aldimine pK$_a$ is greater than 10.5. Additionally, the reaction with one of the substrates, DAPA, is approximately 80% diffusion controlled (Table 3, $k_2/(k_{-1} + k_2) = 0.8$).

Steady-State Kinetics. Stoner and Eisenberg (*8*) found that DAPA synthase exhibits ping-pong kinetics typical of PLP-dependent aminotransferases. They determined a steady-state k_{cat} value of 0.13 s^{-1}, and K_m values of 0.2 mM and 1.2 μM for SAM and KAPA, respectively. The k_{cat} value determined by our HPLC-based assay is significantly lower (0.013 s^{-1}, Table 2). The source of this discrepancy is not clear, but the present value is also consistent with the results obtained in the single-turnover reactions (see below).

Single-Turnover Reactions with SAM and DAPA. The physiological reaction of DAPA synthase can be separated into two half-reactions. First, the PLP form of the enzyme reacts with SAM to produce the keto-acid of SAM (*S*-adenosyl-4-methylthio-2-oxobutanoate) and the PMP form of the enzyme. To complete the reaction, the enzyme-bound PMP reacts with KAPA to produce DAPA and regenerates the PLP enzyme. We have analyzed the first physiological half-reaction and the reverse of the second half-reaction, i.e., the reaction of the PLP enzyme with DAPA to produce KAPA, because the PMP form of the enzyme is not stable.
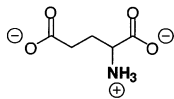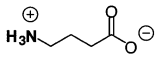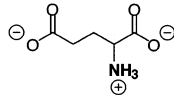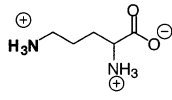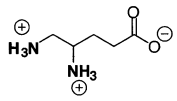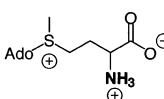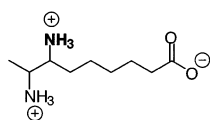
The reactions of the PLP form of the enzyme with SAM and DAPA differ markedly. The apparent K_m for SAM is rather high (300 μM), and the reaction is slow ($k_{max} = 0.016$ s^{-1}), giving a k_{max}/K_m^{app} of 53 M^{-1}s^{-1} (Table 2). Furthermore, a quinonoid intermediate forms rapidly ($k_Q = 47$ s^{-1}) and decays slowly during the reaction with a rate constant equal to k_{max}. In contrast, the apparent K_m for DAPA is low (1 μM), and the reaction occurs faster ($k_{max} = 0.79$ s^{-1}), making k_{max}/K_m^{app} for DAPA more than 10^4-fold greater than that for SAM. No quinonoid intermediate is observed in the reaction with DAPA.

It is likely that the electron-withdrawing sulfonium center of SAM acts to stabilize the anionic quinonoid intermediate in that reaction; thus, it acts as a kinetic trap and slows the overall reaction rate. A stable quinonoid intermediate is also observed during the course of the reaction of SAM with ACC synthase, the only other PLP enzyme known to utilize SAM as a substrate (*32*), although the reaction catalyzed by this enzyme is not an aminotransferase reaction.[3] A similarly electron-withdrawing substrate, cysteine sulfinic acid, has been observed to form a stable quinonoid intermediate when reacted with aspartate aminotransferase (*33*).

Why is SAM uniquely employed by this enzyme as the amino donor? SAM appears to be a poor substrate for transamination as defined by its kinetic constants, and use of SAM for transamination is a waste of a costly metabolite (ATP is converted to adenosine, inorganic phosphate, and pyrophosphate in the process of synthesizing SAM (*34*)). It is interesting to speculate why this enzyme has evolved to utilize SAM. Aminotransferase-catalyzed reactions are most efficient when the pK_a of the substrate and the enzyme are separated (see above). Since these enzymes react with two substrates, the substrates must themselves have similar pK_a's in order for this separation to be achieved in both cases, and SAM may be the only substrate available with an appropriate pK_a. Moreover, biotin is generally synthesized in *E. coli* at a low level (*35*), so the cost in consumption of SAM might not be overly taxing. The only other close connection between biotin synthesis and SAM is that the final enzyme in the biosynthetic pathway, biotin synthase, utilizes SAM as a substrate to form an adenosyl radical (*36*).

Arg391 is Not Required for Binding of the Carboxylate of SAM. Because aminotransferase reactions require that two substrates must bind in succession to the same portion of the cofactor, the active sites of aminotransferases must be dual-specific, i.e., they must be able to selectively bind both substrates. In most cases, both of these substrates are α-amino acids, so the enzyme must accommodate variation only of the side-chain. A small number of aminotransferases, however, effect reactions at substrate positions other than C$_\alpha$. Of these, structures are available only for several enzymes of aminotransferase subclass II (*10*). These include γ-aminobutyrate (GABA) aminotransferase (EC 2.6.1.19), whose substrates are GABA and glutamate (*37*); ornithine aminotransferase (EC 2.6.1.13), which reacts with the δ-amino group of ornithine and the α-amino group of glutamate (*38*); and glutamate 1-semialdehyde aminomutase (GSA; EC 5.4.3.8), which reacts with both the γ- and δ-amino groups of diaminovalerate (*39*). The substrates for these enzymes

Table 4: Substrates of Aminotransferases that Utilize Non-α-Amino Acids

Enzyme	Substrates[a]	
	α-amino acid	non-α-amino acid
GABA ATase		
Ornithine ATase		
GSA[b]		
DAPA synthase		

[a] All substrates are shown as amino acids for clarity. The reactive amino group of each substrate is in boldface. [b] GSA reacts with both amino groups of one substrate and therefore does not require an additional amino donor.

are shown in Table 4. An important question for these enzymes is how they recognize both C$_\alpha$- and non-C$_\alpha$-amino acids, or in the case of ornithine aminotransferase, how the two amino groups on the same substrate are distinguished. GSA is an exception in that it does not utilize an α-amino acid substrate in addition to a non-α-amino acid.

Structural studies and computational modeling provide one answer: in both GABA aminotransferase (*40*, *41*) and ornithine aminotransferase (*42*), the residue structurally equivalent to Arg386 of aspartate aminotransferase (AATase) is used for binding the carboxylate of α-amino acids just as it is in AATase. When the ω-amino acid substrates GABA and ornithine are bound, however, this arginine residue is involved in a salt bridge with a conserved glutamate. The carboxylates of these substrates instead interact with a second arginine elsewhere in the active site. The role of the Arg386 equivalent is thus limited to binding only one of the two substrates.

An early phylogenetic analysis of aminotransferases concluded that four residues are completely conserved—Asp/Glu222 (pig cytosolic AATase numbering), which hydrogen bonds with the pyridinium nitrogen atom of the cofactor; Lys258, which forms the aldimine with PLP; Arg386, which makes a salt bridge with the substrate carboxylate; and Gly197, whose function is unknown. This analysis led to the suggestion that Arg391 of DAPA synthase is equivalent to Arg386 of AATase (*9*). A more recent structural alignment (*3*, *10*) has shown that these two arginine residues do not superimpose. Only one residue (Asp222) is structurally conserved across all of the enzymes in Fold Type I.[4] It now

---

[3] The enzyme lysine 2,3-aminomutase (EC 5.4.3.2) also uses SAM, but not in the reaction with PLP (*2*).

[4] The active site Lys258 (AATase numbering) is functionally conserved, but not structurally because it is shifted out of frame in subclass II (*3*).

appears that there is no equivalent to Arg386 in either DAPA synthase or GSA, based on both the structural comparison and sequence alignments of enzymes within the same subclass (*40, 41*). Although it is expected that GSA might have lost this residue, since it does not bind α-amino acids (Table 4) and this residue appears to be required only for that purpose, DAPA synthase stands out as the first aminotransferase observed to bind an α-amino acid substrate without a residue structurally equivalent to Arg386.

Arg391 does, however, form a salt bridge with the terminal carboxylate of KAPA in the structure of DAPA synthase with that substrate (*3*). When KAPA is not present, this residue is hydrogen-bonded to a glutamine residue. As no structure of the DAPA synthase SAM complex is yet available, we postulated that Arg391 might substitute functionally for Arg386 and interact with the carboxylate of SAM as well as that of KAPA. To investigate this possibility, the R391A mutation was constructed. This replacement results in a large increase in both the steady-state K_m for KAPA and the single-turnover apparent K_m for DAPA (Table 2), confirming the role of this residue in the binding of these substrates. By contrast, the R391A construct exhibits near WT kinetics in the reaction with SAM (Table 2). The identification of an enzyme residue that interacts with the alpha-carboxylate of SAM remains elusive.

ACKNOWLEDGMENT

REFERENCES

1. Lucet, D., Le Gall, T., Mioskowksi, C., Ploux, O., and Marquet, A. (1996) *Tetrahedron: Asymmetry 7*, 985−988.
2. Frey, P. A., Ballinger, M. D., and Reed, G. H. (1998) *Biochem. Soc. Trans. 26*, 304−10.
3. Käck, H., Sandmark, J., Gibson, K., Schneider, G., and Lindqvist, Y. (1999) *J. Mol. Biol. 291*, 857−76.
4. Schneider, G., and Lindqvist, Y. (2001) *FEBS Lett. 495*, 7−11.
5. Marquet, A., Bui, B. T., and Florentin, D. (2001) *Vitam. Horm. 61*, 51−101.
6. Pai, C. H., and McLaughlin, G. E. (1969) *Can. J. Microbiol. 15*, 809−10.
7. Stoner, G. L., and Eisenberg, M. A. (1975) *J. Biol. Chem. 250*, 4029−36.
8. Stoner, G. L., and Eisenberg, M. A. (1975) *J. Biol. Chem. 250*, 4037−43.
9. Mehta, P. K., Hale, T. I., and Christen, P. (1993) *Eur. J. Biochem. 214*, 549−61.
10. Schneider, G., Käck, H., and Lindqvist, Y. (2000) *Struct. Fold. Des. 8*, R1−6.
11. du Vigneaud, V., Melville, D. B., Folkers, K., Wolf, D. E., Mozingo, R., Keresztesy, J. C., and Harris, S. A. (1942) *J. Biol. Chem. 146*, 475−85.
12. Nudelman, A., Nudelman, A., Marcovici-Mizrahi, D., and Flint, D. (1998) *Bioorg. Chem. 26*, 157−168.
13. McCarthy, D. L., Capitani, G., Feng, L., Gruetter, M. G., and Kirsch, J. F. (2001) *Biochemistry 40*, 12276−84.
14. Käck, H., Gibson, K. J., Gatenby, A. A., Schneider, G., and Lindqvist, Y. (1998) *Acta Crystallogr., Sect. D: Biol. Crystallogr. 54*, 1397−8.
15. Onuffer, J. J., Ton, B. T., Klement, I., and Kirsch, J. F. (1995) *Protein Sci. 4*, 1743−9.
16. Kuramitsu, S., Hiromi, K., Hayashi, H., Morino, Y., and Kagamiyama, H. (1990) *Biochemistry 29*, 5469−76.
17. Chen, R. F. (1967) in *Fluorescence* (Guilbault, G. G., Ed.) pp 479−480, Marcel Dekker, Inc., New York.
18. Kuzmic, P. (1996) *Anal. Biochem. 237*, 260−73.
19. Roth, M. (1971) *Anal. Chem. 43*, 882.
20. Contestabile, R., Jenn, T., Akhtar, M., Gani, D., and John, R. A. (2000) *Biochemistry 39*, 3091−6.
21. Leslie, A. G. W. (1992) *Joint CCP4 and ESF-EAMCB Newsletter Protein Crystallography 26*, Daresbury Laboratory, Daresbury, U.K.
22. Evans, P. R. (1993) in *CCP4 Study Weekend on Data Collection and Processing*, pp 114−122, Daresbury Laboratory, Daresbury, U.K.
23. Navaza, J. (1994) *Acta Crystallogr., Sect. A 50*, 157−163.
24. Murshudov, G. N., Vagin, A. A., and Dodson, E. J. (1997) *Acta Crystallogr., Sect. D: Biol. Crystallogr. 53*, 240−258.
25. Jones, T. A., Zou, J. Y., Cowan, S., and Kjeldgaard, M. (1991) *Acta Crystallogr., Sect. A 47*, 100−119.
26. Laskowski, R. A., McArthur, M. W., Moss, D. S., and Thornton, J. M. (1993) *J. Appl. Crystallogr. 26*, 282−291.
27. Eisenberg, M. A., and Stoner, G. L. (1971) *J. Bacteriol. 108*, 1135−40.
28. Klee, W. A., and Mudd, S. H. (1967) *Biochemistry 6*, 988−98.
29. Li, Y., Feng, L., and Kirsch, J. F. (1997) *Biochemistry 36*, 15477−88.
30. Eliot, A. C., and Kirsch, J. F. (2002) *Biochemistry 41*, 3836−42.
31. Gibson, K. J., Lorimer, G. H., Rendina, A. R., Taylor, W. S., Cohen, G., Gatenby, A. A., Payne, W. G., Roe, D. C., Lockett, B. A., Nudelman, A., et al. (1995) *Biochemistry 34*, 10976−84.
32. Feng, L., Geck, M. K., Eliot, A. C., and Kirsch, J. F. (2000) *Biochemistry 39*, 15242−9.
33. Furumo, N. C., and Kirsch, J. F. (1995) *Arch. Biochem. Biophys. 319*, 49−54.
34. Markham, G. D., Hafner, E. W., Tabor, C. W., and Tabor, H. (1983) *Methods Enzymol. 94*, 219−22.
35. Pai, C. H. (1972) *J. Bacteriol. 112*, 1280−7.
36. Guianvarc'h, D., Florentin, D., Tse Sum Bui, B., Nunzi, F., and Marquet, A. (1997) *Biochem. Biophys. Res. Commun. 236*, 402−6.
37. Bloch-Tardy, M., Rolland, B., and Gonnard, P. (1974) *Biochimie 56*, 823−32.
38. Peraino, C., Bunville, L. G., and Tahmisian, T. N. (1969) *J. Biol. Chem. 244*, 2241−9.
39. Smith, M. A., Kannangara, C. G., Grimm, B., and von Wettstein, D. (1991) *Eur. J. Biochem. 202*, 749−57.
40. Toney, M. D., Pascarella, S., and De Biase, D. (1995) *Protein Sci. 4*, 2366−74.
41. Storici, P., Capitani, G., De Biase, D., Moser, M., John, R. A., Jansonius, J. N., and Schirmer, T. (1999) *Biochemistry 38*, 8628−34.
42. Storici, P., Capitani, G., Müller., R., Schirmer, T., and Jansonius, J. N. (1999) *J. Mol. Biol. 285*, 297−309.
43. Kraulis, P. J. (1991) *J. Appl. Crystallogr. 24*, 946−50.
44. Esnouf, R. M. (1997) *J. Mol. Graphics Modelling 15*, 133−138.
45. Merritt, E. A., and Bacon, D. J. (1997) *Methods Enzymol. 277*, 505−524.